Supplementary Information

Inhibition of Death-associated Protein Kinase 1 Attenuates *Cis* P-tau and Neurodegeneration in Traumatic Brain Injury

Kim et al.

Antibodies	Dilutions	Source	Identifier	Specificity
Mouse anti-DAPK1	1:1000 (WB)	MilliporeSigma	D2178	[*Kim et al., 2014*]
Rabbit anti-DAPK1	1:50-100 (IF)	MilliporeSigma	SAB4500620	[*Zhang et al., 2014*]
Mouse anti-β-actin	1:20000 (WB)	MilliporeSigma	A3854	[*Guglielmotto et al., 2014*]
Mouse anti-*cis* P-tau	1:1000 (WB) 1:250 (IF)	Kun Ping Lu	[*Kondo et al., 2015*]	[*Kondo et al., 2015*]
Mouse anti-p-tau (T231)	1:10000 (WB) 1:250 (IF)	Abcam	ab151559	[*Fang et al., 2019*]
Mouse anti-Tau	1:2000 (WB)	Santa Cruz Biotechnology	sc-58860	[*Ittner et al., 2009*]
Rabbit pS71-Pin1	1:2000-1:5000 (IF)	Kun Ping Lu	[*Lee et al., 2011*]	[*Lee et al., 2011*]
Mouse Pin1	1:1000 (IF)	Kun Ping Lu	[*Lee et al., 2011*]	[*Lee et al., 2011*]
Rabbit Pin1	1:500 (IF)	Kun Ping Lu	[Ryo et al., 2003]	[Ryo et al., 2003]
Rabbit anti-GFAP	1:500 (IF)	Abcam	ab7260	[*Albayram et al., 2017*]
Rabbit anti-Iba-1	1:500 (IF)	Wako	019-19741	[*Albayram et al., 2017*]
Rabbit anti-T22	1:1000 (IF)	MilliporeSigma	ABN454	[*Lasagna-Reeves et al., 2012*]
Mouse anti-AT8	1:200 (IF)	Thermo Fisher Scientific	MN1020	[*Albayram et al., 2017*]
Mouse anti-AT100	1:500 (IF)	Thermo Fisher Scientific	MN1060	[*Albayram et al., 2017*]
Rabbit anti-MAP2	1:250 (IF)	Abcam	ab32454	[Huh *et al., 2003*]
Mouse anti-NeuN	1:500 (IF)	MilliporeSigma	MAB377	[*Albayram et al., 2017*]

Supplemental Table S1. Primary antibodies used in this study

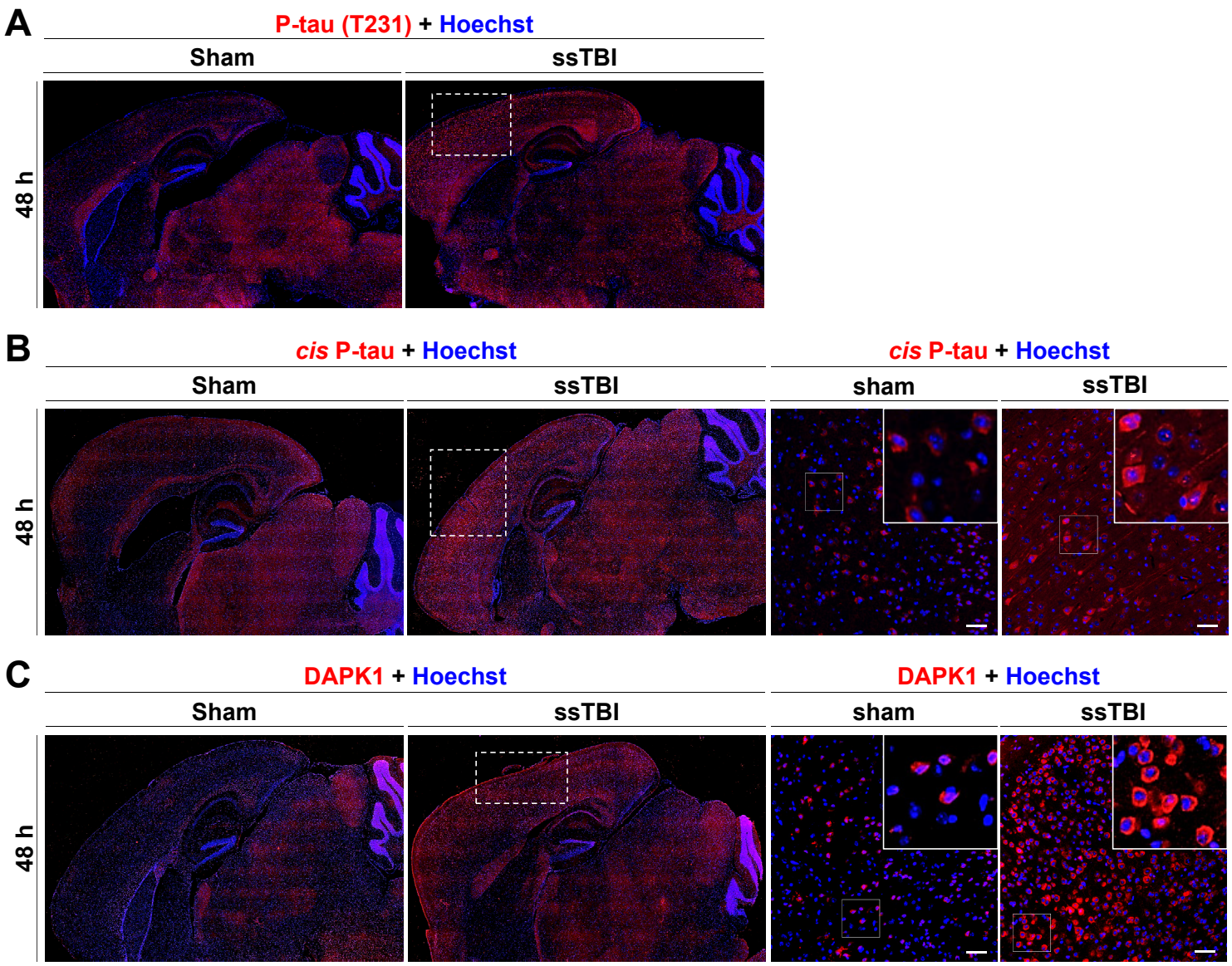

Supplemental Fig. S1. ssTBI induces significant induction of *cis* P-tau at Thr231 and DAPK1 in mouse brains. Mice were subjected to ssTBI by weight drop. A-C. The sagittal section of mouse brains were subjected to immunofluorescence staining to detect P-tau (T231) (A), *cis* P-tau (B) and DAPK1 (C). P-tau (T231), *cis* P-tau, DAPK1, red; DNA, blue. Rectangle indicates the injured area by weight drop. Experiments were performed in triplicate with at least three mice per group per experiment.

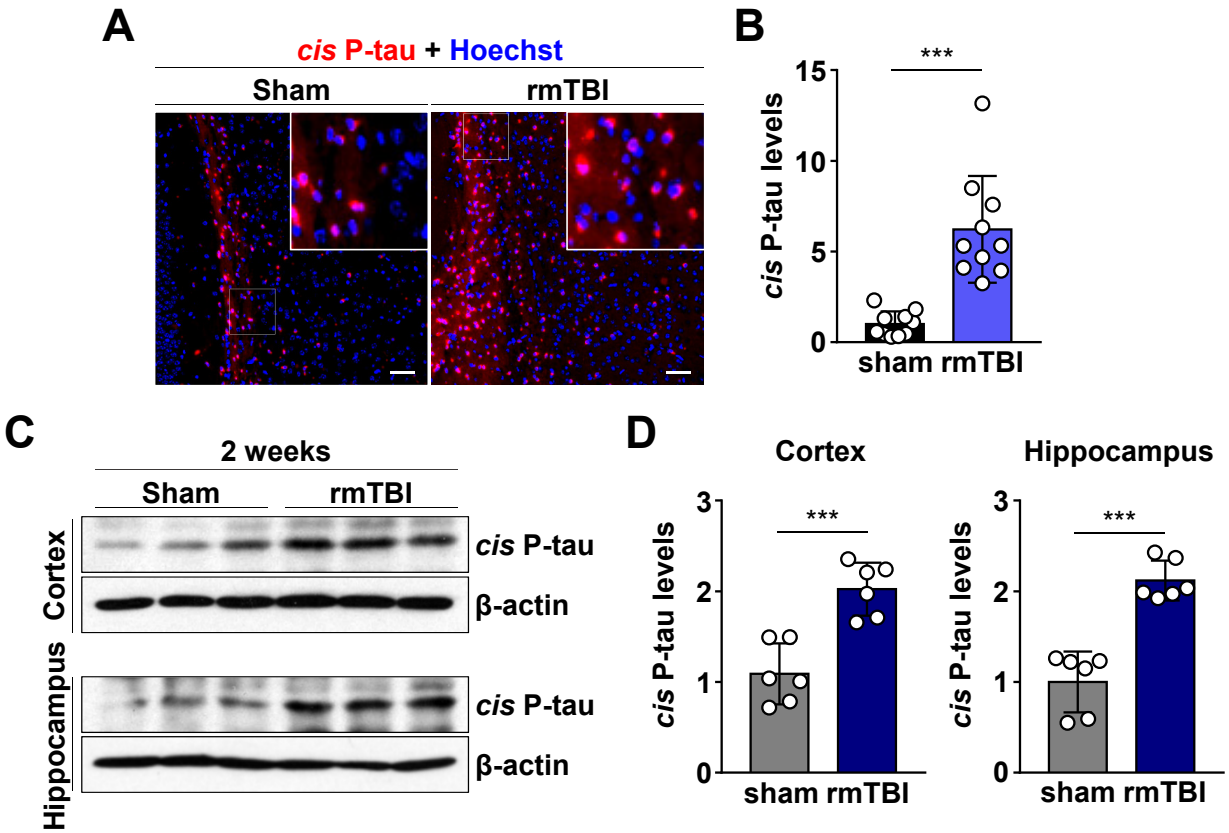

Supplemental Fig. S2. rmTBI induces significant induction of *cis* P-tau in mouse brains. Mice were subjected to rmTBI by weight drop with a weight of 54 grams dropped from a height of 32 inches. For the impact of rmTBI, the mouse heads were injured once a day for 5 days to induce rmTBI. A-B. The mouse brains were collected immediately after the fifth injury, and subjected to immunofluorescence staining (A) to detect *cis* P-tau. *cis* P-tau, red; DNA, blue. Scale bar= 50 μm. The images of *cis* P-tau immunostaining were quantified and analyzed using two-tailed paired t-tests (B). C-D. Two weeks after rmTBI, mouse brains were collected for immunoblotting (C) to detect *cis* P-tau induction in the cerebral cortex and hippocampus. *cis* P-tau protein levels in the cerebral cortex and hippocampus were quantified and analyzed using *cis* P-tau/β-actin ratio (D). Statistical significances were determined by two-tailed paired t-tests. The results shown are the mean ± SD (***$p<0.001$). Experiments were performed in duplicate with at least three mice per group per experiment.

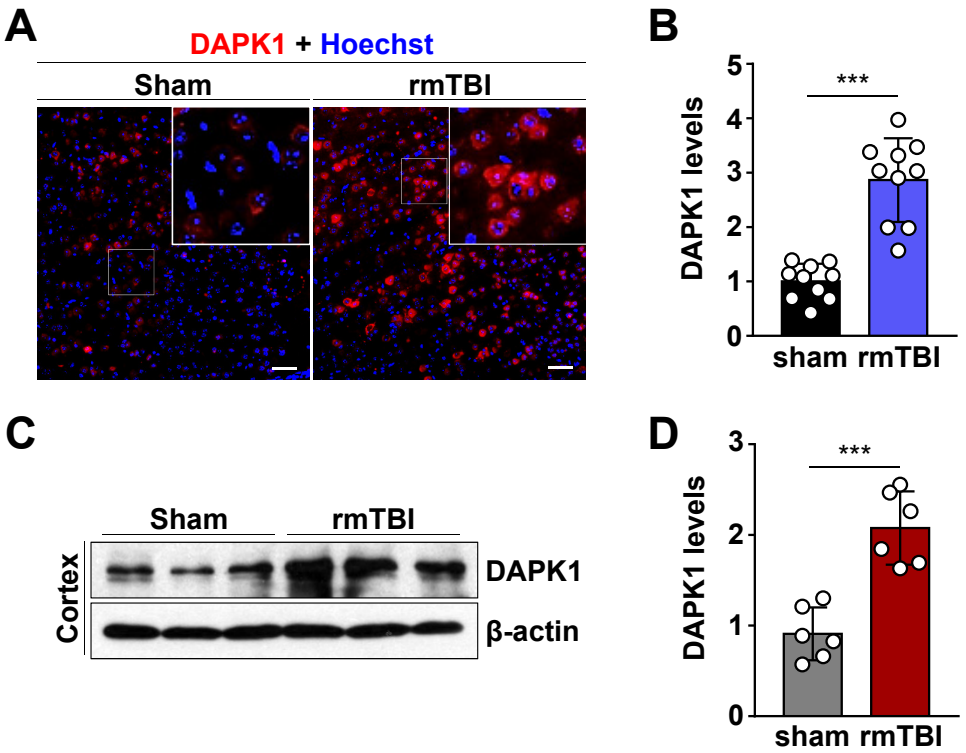

Supplemental Fig. S3. rmTBI induces expression of DAPK1 in mouse brains. A-B. The rmTBI mouse brains were collected immediately after the fifth injury, and DAPK1 was detected by immunofluorescence. DAPK1, red; DNA, blue. Scale bar= 50 μm. The images of DAPK1 were quantified and analyzed using two-tailed paired t-tests (B). C. After rmTBI, the mice were subjected to immunoblotting to detect DAPK1 expression in the cerebral cortex. D. The DAPK1 expression levels in the cerebral cortex was calculated as the DAPK1/β-actin ratio. Statistical significance was determined by two-tailed Student's t-test. The results shown are the mean ± SD (***$p<0.001$). Experiments were performed in duplicate with at least three mice per group per experiment.

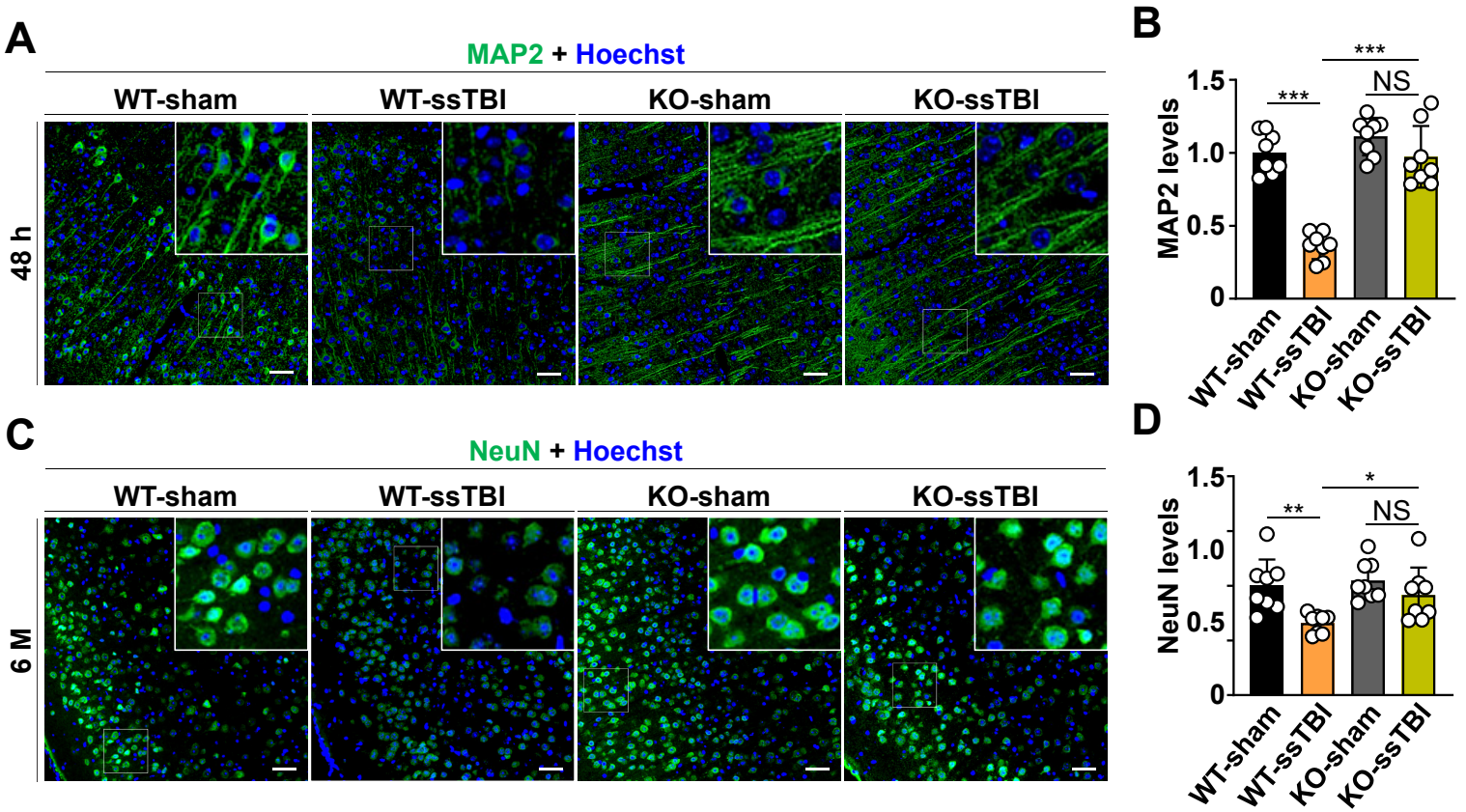

Supplemental Fig. S4. Eliminating DAPK1 prevents acute neuronal injury and chronic neuronal loss after ssTBI. A. TBI-injured WT and DAPK1 KO mouse brains were harvested at 48 h and analyzed by immunofluorescence with a MAP2 antibody. MAP2, green; DNA, blue. B. Quantification of MAP2 immunostaining at 48 h; p-values for MAP2 was calculated using one-way ANOVA with Tukey's multiple comparisons test. C. WT and DAPK1 KO mouse brains were collected at 6 months after injury, and NeuN was detected by immunofluorescence. NeuN, green; DNA, blue. D. The images of NeuN immunostaining were quantified and analyzed using one-way ANOVA with Tukey's multiple comparisons test. The results shown are the mean ± SD (***$p<0.001$, **$p<0.01$, *$p<0.05$). Experiments were performed in triplicate with at least three mice per group per experiment. Scale bar= 50 μm. NS, no significance.

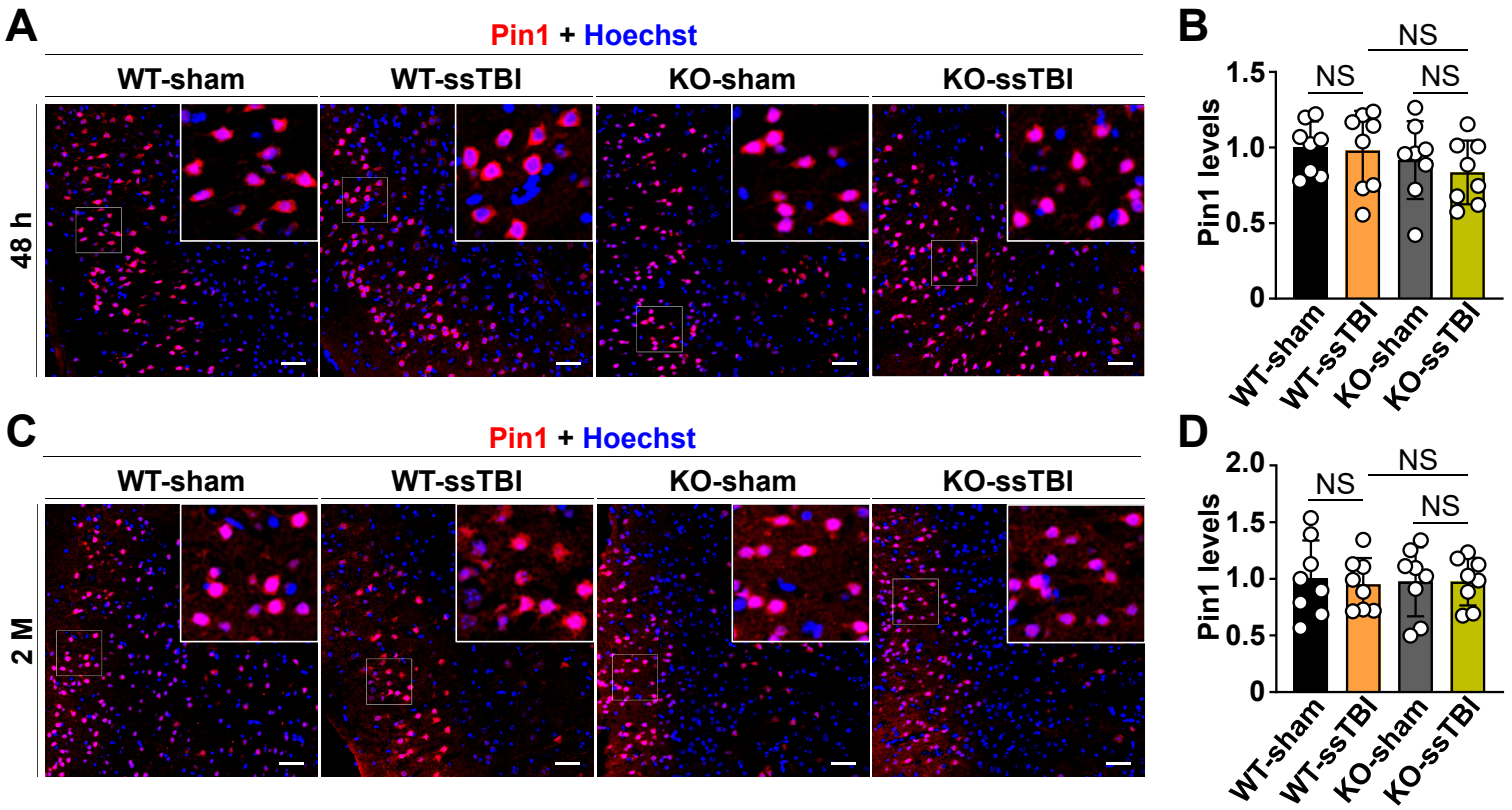

Supplemental Fig. S5. ssTBI does not affect pin1 expression in the cerebral cortex. A-D. TBI-injured WT and DAPK1 KO mouse brains were harvested at 48 h (A, B) and 2 months (C, D) and were analyzed by immunofluorescence with a Pin1 antibody. Pin1, red; DNA, blue. Quantification of Pin1 immunostaining at 48 h (B) and 2 months (D); p-values for Pin1 were calculated using one-way ANOVA with Tukey's multiple comparisons test. The results shown are the mean ± SD. Experiments were performed in triplicate with at least three mice per group per experiment. Scale bar= 50 μm. NS, no significance.

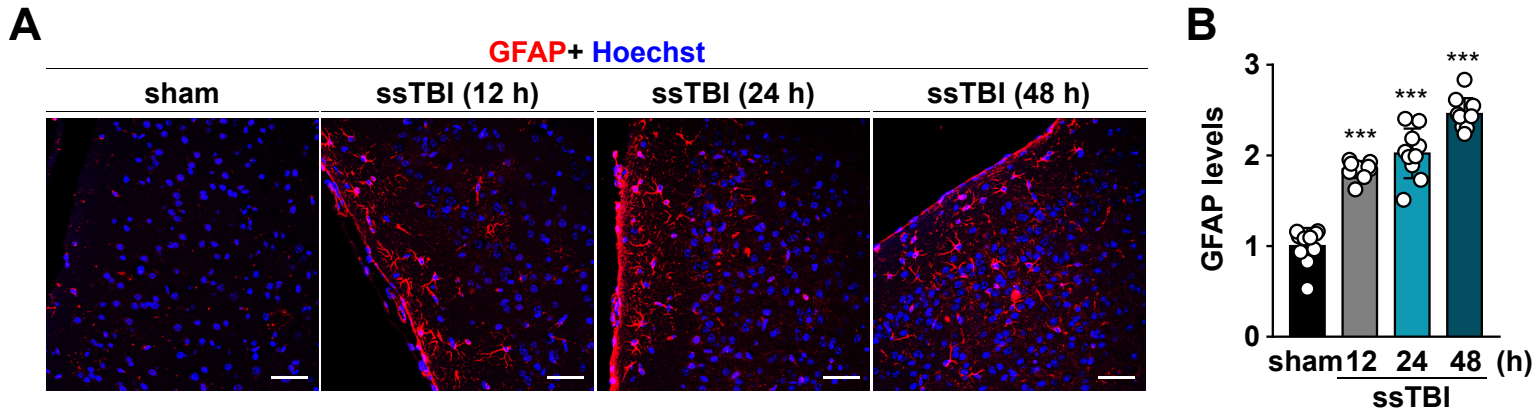

Supplemental Fig. S6. TBI acutely induces neuroinflammation in time dependent manner in the cerebral cortex. A. GFAP expression in the cerebral cortex increased in a time-dependent manner in WT mice after TBI examined by immunofluorescence staining. GFAP, red; DNA, blue. Scale bar= 50 μm. B. Quantification of GFAP in cortex; p-values for GFAP was calculated using one-way ANOVA with Tukey's multiple comparisons test. The results shown are the mean ± SD (***$p<0.001$). Experiments were performed in triplicate with at least three mice per group per experiment.

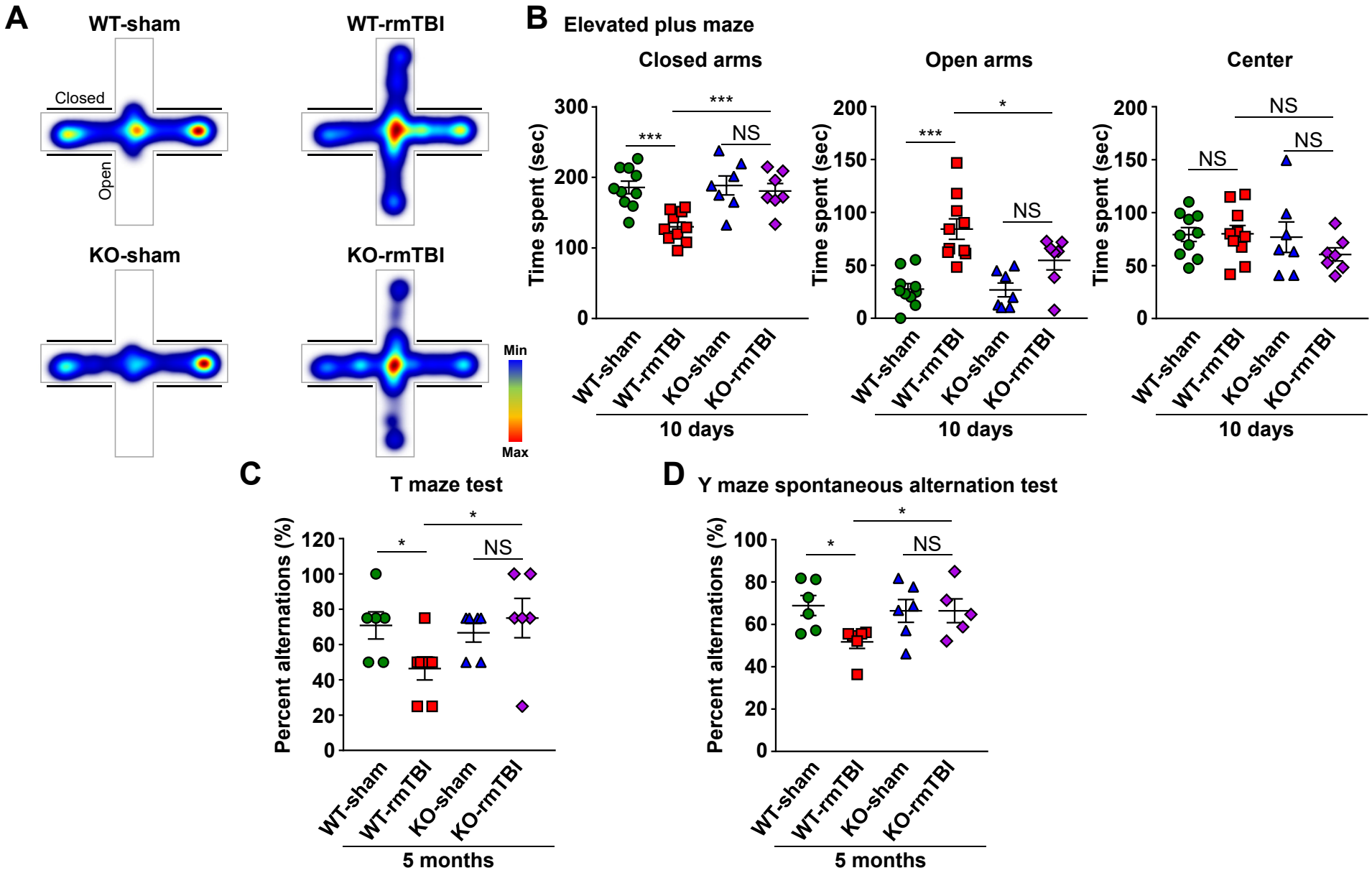

Supplemental Fig. S7. DAPK1 KO reverses rmTBI-induced behavioral impairments in mice. A, B. rmTBI-injured mice were subjected to the elevated plus maze test (n= 7-10), and the time spent in the three arms was measured and quantified. C. T maze test was performed to measure spatial working memory at 5 months (n= 6-7) after rmTBI. The behavior results were quantified as a ratio of percentage alternations. D. Y maze spontaneous alternation test was performed to measure spatial leaning and working memory at 5 months (n= 5-6) after rmTBI. The Y maze behavior results were quantified as a ratio of percentage alternations. The p-values of all the representative data were calculated using one-way ANOVA with Tukey's multiple comparisons test; All the results shown are the mean ± SEM (***p<0.001, *p<0.05). NS, no significance.

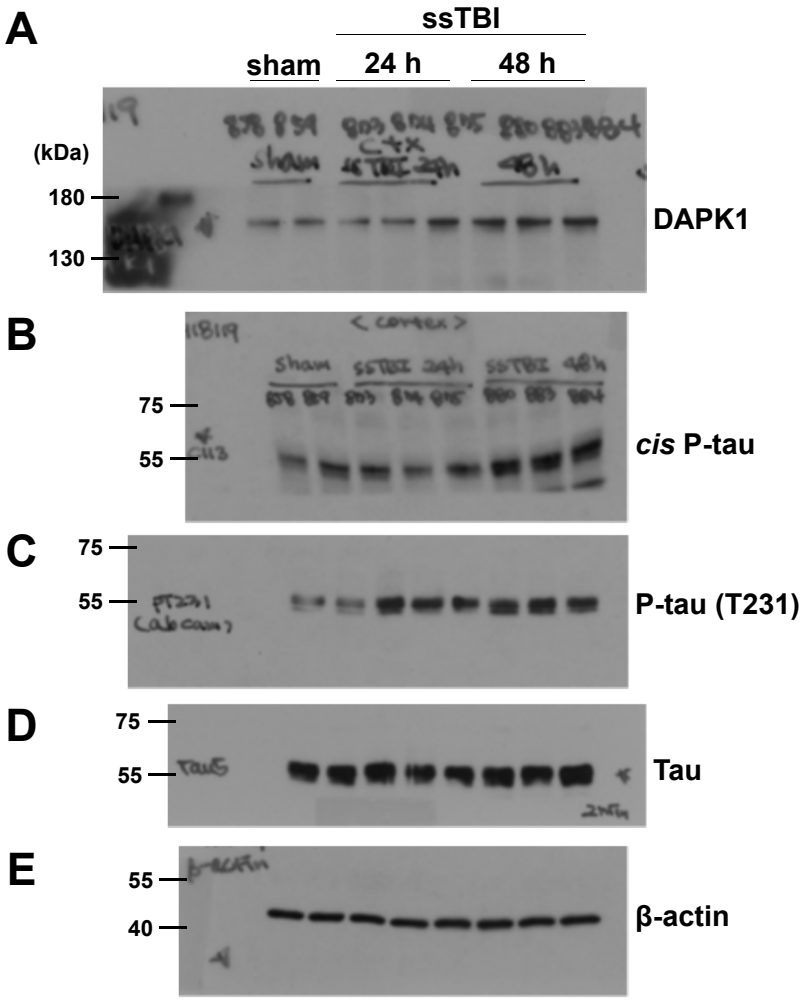

Supplemental Fig. S8. Uncropped immunoblotting images for Fig. 1.

The PVDF membranes were cut to fit the molecular size of antibodies. Related to Fig. 1G.

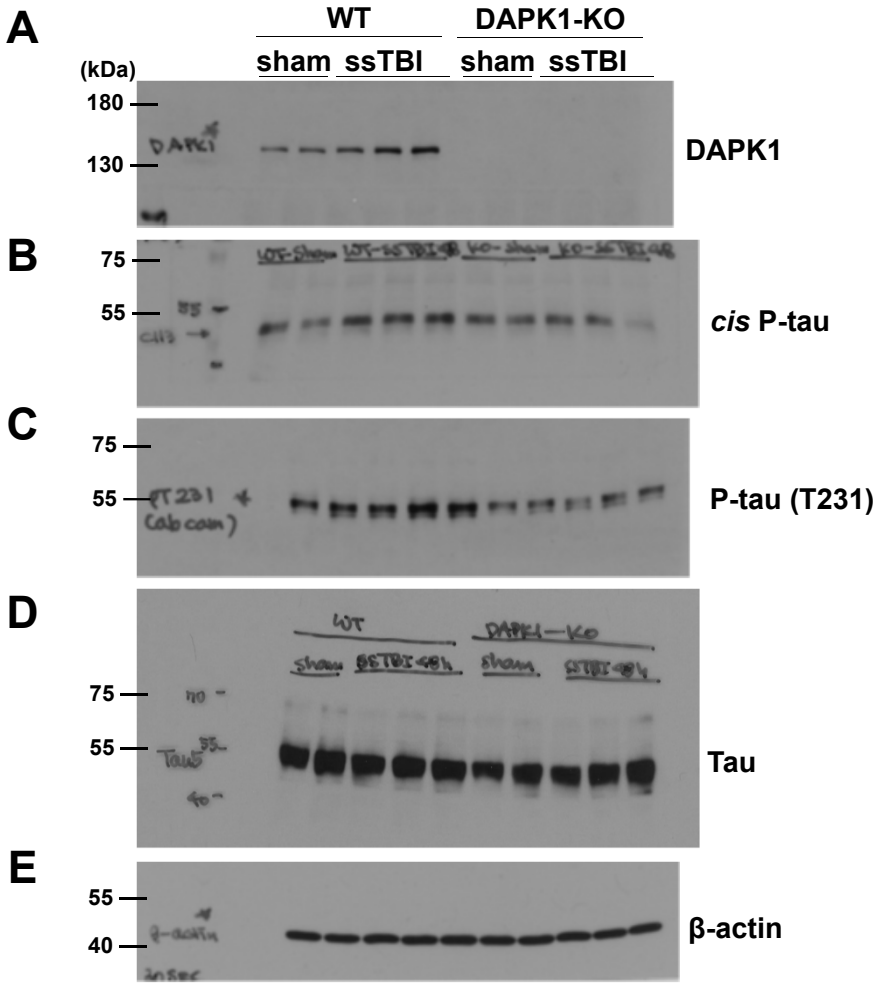

Supplemental Fig. S9. Uncropped immunoblotting images for Fig. 2

The PVDF membranes were cut to fit the molecular size of antibodies. All images related to Fig. 2I.

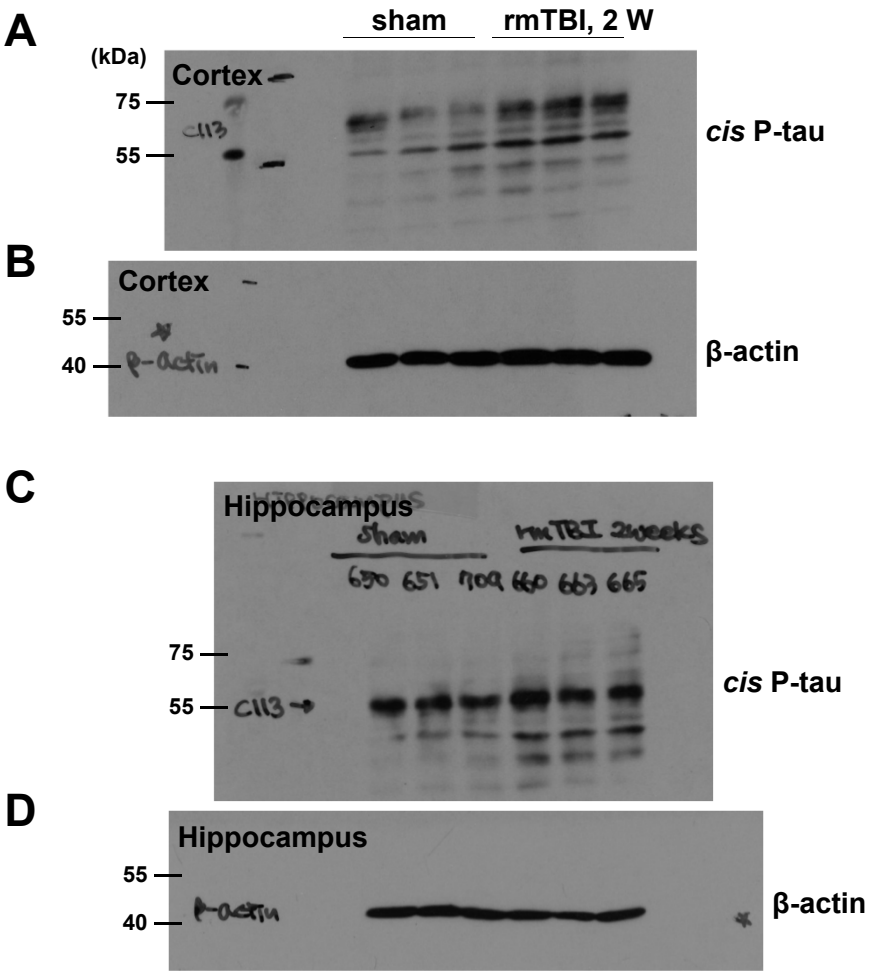

Supplemental Fig. S10. Uncropped immunoblotting images for Supplemental Fig. S2.

The PVDF membranes were cut to fit the molecular size of antibodies. All images related to Supplemental Fig. S2C.

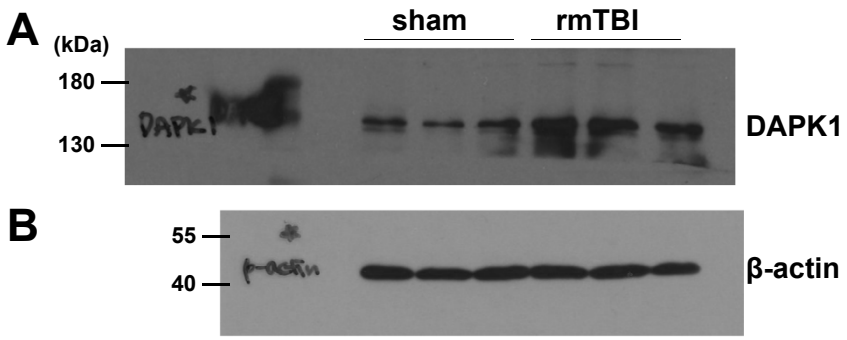

Supplemental Fig. S11. Uncropped immunoblotting images for Supplemental Fig. S3.

The PVDF membranes were cut to fit the molecular size of antibodies. All images related to Supplemental Fig. S3C.

Supplementary references

1. Albayram, O., Kondo, A., Mannix, R., Smith, C., Tsai, C.Y., Li, C., Herbert, M.K., Qiu, J., Monuteaux, M., Driver, J., Yan, S., Gormley, W., Puccio, A.M., Okonkwo, D.O., Lucke-Wold, B., Bailes, J., Meehan, W., Zeidel, M., Lu, K.P., Zhou, X.Z., 2017. Cis P-tau is induced in clinical and preclinical brain injury and contributes to post-injury sequelae. *Nature communications* 8**,** 1000.

2. Fang, E.F., Hou, Y., Palikaras, K., Adriaanse, B.A., Kerr, J.S., Yang, B., Lautrup, S., Hasan-Olive, M.M., Caponio, D., Dan, X., Rocktaschel, P., Croteau, D.L., Akbari, M., Greig, N.H., Fladby, T., Nilsen, H., Cader, M.Z., Mattson, M.P., Tavernarakis, N., Bohr, V.A., 2019. Mitophagy inhibits amyloid-beta and tau pathology and reverses cognitive deficits in models of Alzheimer's disease. *Nat Neurosci* 22**,** 401-412.

3. Guglielmotto, M., Monteleone, D., Piras, A., Valsecchi, V., Tropiano, M., Ariano, S., Fornaro, M., Vercelli, A., Puyal, J., Arancio, O., Tabaton, M., Tamagno, E., 2014. Abeta1-42 monomers or oligomers have different effects on autophagy and apoptosis. *Autophagy* 10**,** 1827-1843.

4. Huh, J.W., Raghupathi, R., Laurer, H.L., Helfaer, M.A., Saatman, K.E., 2003. Transient loss of microtubule-associated protein 2 immunoreactivity after moderate brain injury in mice. *J Neurotrauma* 20**,** 975-984.

5. Ittner, L.M., Ke, Y.D., Gotz, J., 2009. Phosphorylated Tau interacts with c-Jun N-terminal kinase-interacting protein 1 (JIP1) in Alzheimer disease. *J Biol Chem* 284**,** 20909-20916.

6. Kim, B.M., You, M.-H., Chen, C.-H., Lee, S., Hong, Y., Hong, Y., Kimchi, A., Zhou, X.Z., Lee, T.H., 2014. Death-associated protein kinase 1 plays a critical role in aberrant tau protein regulation and function. *Cell Death Dis* 5**,** e1237.

7. Kondo, A., Shahpasand, K., Mannix, R., Qiu, J., Moncaster, J., Chen, C.H., Yao, Y., Lin, Y.M., Driver, J.A., Sun, Y., Wei, S., Luo, M.L., Albayram, O., Huang, P., Rotenberg, A., Ryo, A., Goldstein, L.E., Pascual-Leone, A., McKee, A.C., Meehan, W., Zhou, X.Z., Lu, K.P., 2015. Antibody against early driver of neurodegeneration cis P-tau blocks brain injury and tauopathy. *Nature* 523**,** 431-436.

8. Lasagna-Reeves, C.A., Castillo-Carranza, D.L., Sengupta, U., Sarmiento, J., Troncoso, J., Jackson, G.R., Kayed, R., 2012. Identification of oligomers at early stages of tau aggregation in Alzheimer's disease. *Faseb J* 26**,** 1946-1959.

9. Lee, T.H., Chen, C.-H., Suizu, F., Huang, P., Schiene-Fischer, C., Daum, S., Zhang, Y.J., Goate, A., Chen, R.-H., Zhou, X.Z., Lu, K.P., 2011. Death associated protein kinase phosphorylates Pin1 and inhibits its prolyl isomerase activity and cellular function. *Mol. Cell***,** In press.

10. Ryo, A., Suizu, F., Yoshida, Y., Perrem, K., Liou, Y.C., Wulf, G., Rottapel, R., Yamaoka, S., Lu, K.P., 2003. Regulation of NF-kappaB signaling by Pin1-dependent prolyl isomerization and ubiquitin-mediated proteolysis of p65/RelA. *Mol Cell* 12**,** 1413-1426.

11. Zhang, J., Hu, M.M., Shu, H.B., Li, S., 2014. Death-associated protein kinase 1 is an IRF3/7-interacting protein that is involved in the cellular antiviral immune response. *Cell Mol Immunol* 11**,** 245-252.